29th Congress of the International Council of the Aeronautical Sciences
St. Petersburg, Russia; September 7-12, 2014

HYPERSONIC FLOWFIELD AND HEAT FLUX PECULIARITIES ON THE NEW SPACE LAUNCHER WITH WINGED REUSABLE FIRST STAGE.

S.M. Drozdov*, V.N. Brazhko*, V.E. Mosharov*, A.S. Skuratov*, D.S. Fedorov*, V.V. Gorbatenko, P.A. Lehov**, J.N. Chibisov****
*** TsAGI, ** KSRPSC**

Keywords: *space launcher, winged module, hypersonic flow.*

Abstract

The main purpose of this work is to investigate experimentally under hypersonic velocities the features of the flow field structure and the heat flux distribution on the new space launcher with two attached winged modules and on the separated winged module of the first stage. It is important to determine regions and elements of vehicle layout subjected to increased aerodynamic and heat loads, to develop methods and means for vehicle layout protection against the loads obtained.

The following investigations are performed in the experiments at TsAGI wind tunnels T-117 and UT-1M: investigations of surface heat flux by means of thermo sensitive coatings (melting paints) at T-117; investigations of surface heat flux by TSP-method (temperature sensitive paint - luminophor) at UT-1M and schlieren flow visualization.

1 Introduction

Currently an active research is carried out in Russia concerning the designing of launch vehicles of new generation (LV). Along with the "Angara" single-used rocket the Khrunichev State Research and Production Space Center (KSRPSC) develops a principally new Space Launcher with a Winged Reusable First Stage (SLWRFS). The Central Aerohydrodynamic Institute (TsAGI) actively participates in this project in the scope of aerodynamic and heat testing, numerical flow simulation over LV, flight dynamic analysis of LV and strength tests.

The investigations were carried out according to the contract with the KSRPSC in compliance with statement of work of ROSCOSMOS (Federal Space Agency of the Russian Federation) for the designing process "Development of Reusable Space-Rocket System of the first generation (RSRS-1)". The RSRS-1 is intended for multipurpose application: spacecraft launching to the orbits of different heights and inclinations, for the launch of manned vehicles and for the fundamental minimization of the regions where the separated parts and debris fall.

Payload of RSRS-1 on a low base orbit of height of 200 km and of inclination of 51.7 will be 25-35 tones. The RSRS-1 under consideration combines elements, principals and technologies, traditional both for space-rocket technology and for aviation. The main feature of the RSRS-1 is the return and automatic landing of the reusable I-stage which is the two winged reusable rocket modules (WRRM). Thus RSRS-1 will be launched as rocket system but return and land like an airplane.

The layout of the new LV distinguishes by usage of the multimodule scheme with a parallel assembly of the winged lateral modules having the sizes comparable to the central module (the packet layout). Such a scheme produces the serious problems of aerodynamic interference of the modules at the launching phase, when the regions of peak aerodynamic loads appear at the LV structure, which frequently have unsteady behavior. In a hypersonic range of velocities the aerodynamics problems of these complicated layouts are aggravated by heat loads which are also characterized by the regions of peak loads.

After separation of SLWRFS at height of 45-50 km, the winged RRM are returned and decelerate in atmosphere from hypersonic ($M\approx7$) to subsonic velocity ($M\approx0.7$). Then they fly back using air breathing engine and land on the aerodrome. The provision of multiple and sufficiently long flights of WRRM at hypersonic velocities requires pretty accurate knowledge about aerodynamics and heat loads peculiarities of the vehicle.

The purpose of this work is the experimental determination of hypersonic flow features and heat transfer on the models of the prospective launch vehicle SLWRFS and of its winged modules RRM, the determination of regions and structural elements exposed to the high heat loads and development of recommendations about protection of LV against these loads.

2 Test models and facilities

Three models were manufactured in the KSRPSC and supplied to TsAGI for testing. This is a heat model of WRRM of a scale of 1/150, the model material is the plastic - polysulfone. The model length is L_{RRM}=223 mm, the wing span is H=136 mm, the model body diameter is D_{RRM}=33.3 mm. The model has three variants of wing with different angles of elevons deflection. The heat model of SLWRFS is the assembly of central module (CM) and two lateral modules WRRM (WRRM+CM+WRRM). It is made at scale 1/150 from plastic - polysulfone. The model length L_{SLWRFS} =443 mm, the wing span is H=136 mm, diameters of the body D_1=33.3 mm and D_2=36.7 mm. Models *1* and *2* are installed in the test section of the UT-1M shock tunnel on a supporting device (fig.1).

Fig.1 Full launcher model in the UT-1M shock tunnel test section

The third model is the heat model of WRRM of a scale of 1/80, (material plastic - polysulfone) is intended for the tests in the T-117 wind tunnel. The model has three variants of a wing with different angles of elevons deflection.

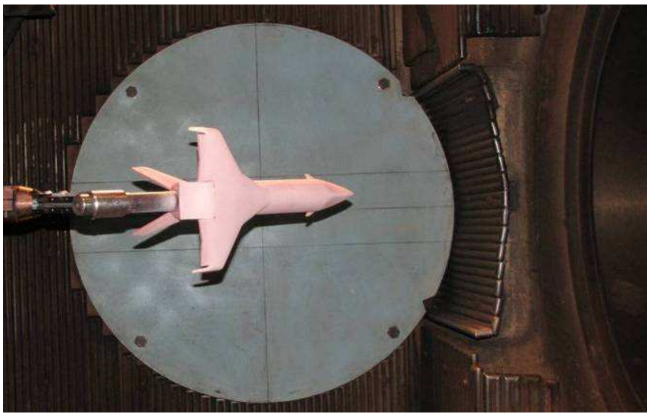

Fig.2 Model of the winged first stage WRRM in the T-117 WT test section.

The tests were carried out in the UT-1M shock tunnel of TsAGI at the Mach number M_∞=6 and in the T-117 large hypersonic wind tunnel of TsAGI at M_∞=7.5. The following experimental methods were applied, namely, the flowfield visualization (the schlieren visualization method or interferometer); the heat flux measurements on the model by melting-paint method or by TSP-method (temperature sensitive paint - luminophor).
For the heat flux computation the temperature distribution T(*t*) on the model surface (obtained at a specified moment of time t after the model injection to the flow) and the analytical solution of one-dimensional heat transfer equation for a semi-infinite body are used.

$$\vartheta = 1 - \exp(\beta^2)\mathrm{erfc}(\beta) \qquad (1)$$

$$\vartheta = [T(t) - T_{in}]/[T_r - T_{in}]$$

Here T_r is the recovery temperature which is taken to be equal to the stagnation temperature $T_r \approx T_0$, T_{in} is the model temperature at t=0.

Heat flux is calculated from equation:

$$q = \frac{\beta(T_o - T_{in})\sqrt{\lambda c \rho}}{\sqrt{t}} \qquad (2)$$

According to the generally accepted method the results of the heat flux measurements on the model surface are presented in a dimensionless form $Q=q/q_o$, where q_o is the heat flux value in the forward stagnation point of a spherical bluntness of the model nose with radius *r*, calculated by the Fay-Riddel formula.

3. Results and discussion

Let us consider some of the most interesting results of the investigations. In Figure 3 one can see the flow picture over the WRRM+CM+WRRM total assembly and the dimensionless heat flux distribution Q along its surface (obtained by the TSP method). It is seen that the head part of the central module of the WRRM+CM+WRRM assembly is not affected by WRRM. On the inverse cone of the head part the rarefaction sector is realized, and the inverse cone is continuously streamlined (without separation). The boundary layer is sufficiently thick – in front of the inverse cone $\delta/R=0.1$, and after the inverse cone $\delta/R=0.15$ (where R=16.7 mm is the radius of the basic part of the inverse cone).

In the zone of aerodynamic interference of the modules the head shock wave from the fairing of CM, from the nose fairing of WRRM and the shock waves from the forward planes are clearly seen. Also the boundary layer on CM and the rarefaction sector on the inverse cone of CM that drops on the nose part of WRRM are designated. The head shock wave almost attached to WRRM nose, there is no flow separation on CM body that could be caused by the presence of WRRM. That confirms the well-chosen shape of the head part of WRRM. In the gap between WRRM and CM there are no shock waves, the channel is not closed, probably, the smooth spreading in front of the connection leg of WRRM with CM occurs.

The heat flux distribution $Q=q/q_o$ on the surface of the model of the WRRM+CM+WRRM assembly at M=6, $\alpha=0$, $\delta л=\delta п=0$ is shown from the side view in Figure 3b. In addition to the peak values on the wing edges, on forward planes and fins, the attention should be paid to the significant levels of heat flux $Q\approx0.1$ on the body of CM, caused by the incidence of shock waves, by the reattachment of vortices and aerodynamic interference from the elements of WRRM. The flow pattern over the WRRM model and the heat flux Q distribution on its surface obtained in the UT-1M shock tunnel for the trajectory Mach number M=6, the Reynolds number $Re\approx9\times10^6$ and for the angle of attack $\alpha=50°$ are shown in Figure 4. It can be seen that the highest value Q=0.75 is achieved in the narrow cross-section region on the lower surface of the center wing section. The reason of this peak heat flux appearance is the internal shock wave closing the supersonic flow between the head shock wave and the model body (Figure 4a). It should be noted that the entire lower surface of the center wing section is subjected to significant heat loads $Q=[0.4 \div 0.5]$. The same level of Q is registered on the wing edges. On the narrow lower rib of the nose fairing the heat flux peak Q=0.42 is realized, and on the "cheeks" there are band peaks up to Q=0.4. The sufficiently high heat flux level of $Q\approx0.35$ is found on the cylindrical part of the model body and on the deflected elevons.

The similar results are obtained by the melting-paint method in the T-117 wind tunnel at M=7.5 , $Re\approx9\times10^6$ on the WRRM model of a scale of 1/80 (Figure 3).

Due to the investigations performed the main peculiarities of the flow over the SLWRFS and the zones of the high heat flux requiring heat protection were determined.

Russia, Moscow region.
Town: Zhukovsky
Zhukovsky Str.1.
CENTRAL AEROHYDRODYNAMIC INSTITUTE (TsAGI).
mailto: smdrozdov@yandex.ru

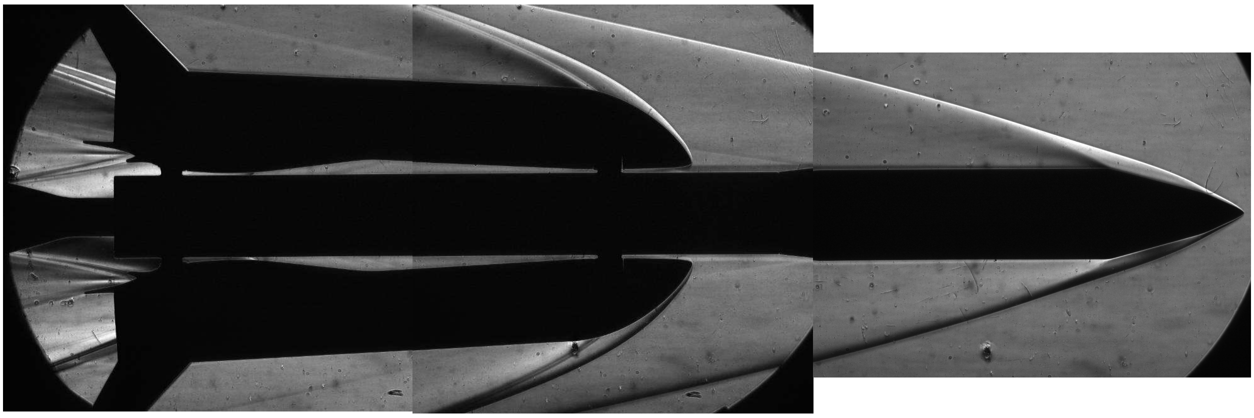

a) flow visualization

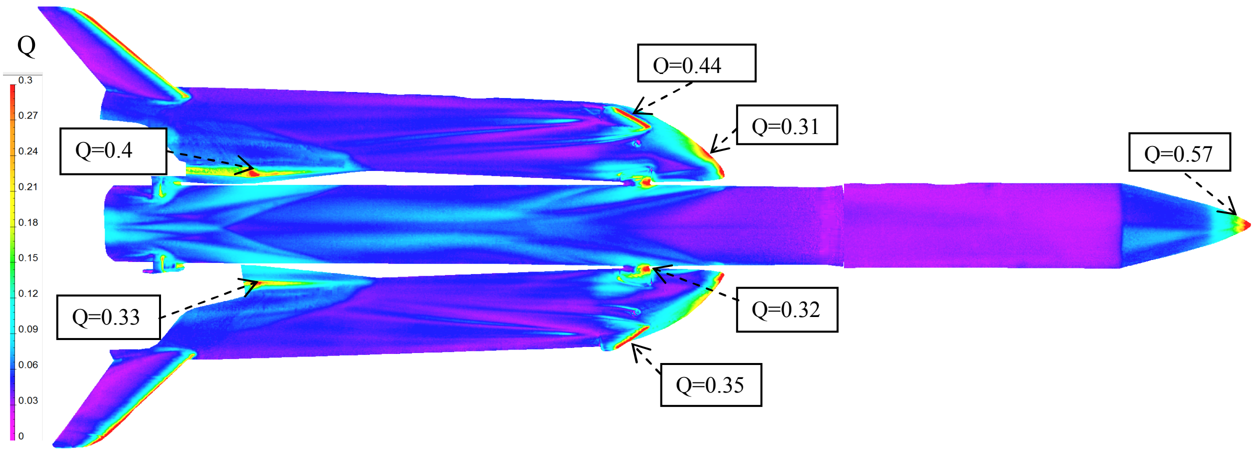

b) heat flux distribution

Figure 3. Tests of the WRRM+CM+WRRM assembly in the UT-1M wind tunnel at α=0 , M=6 , Re≈9×10^6

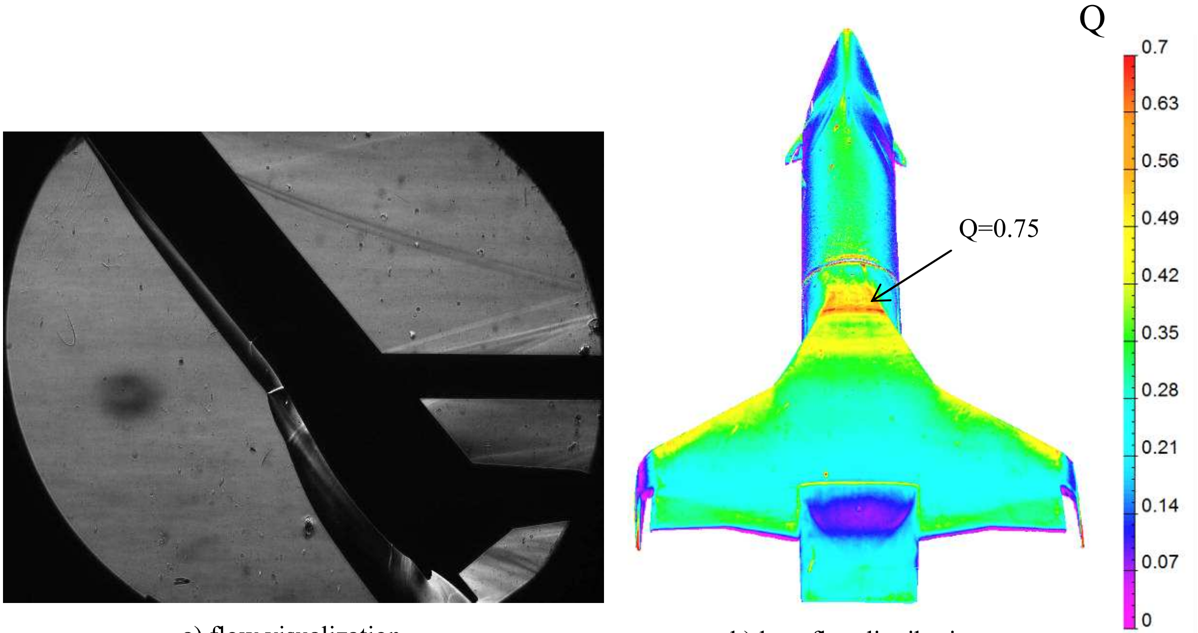

a) flow visualization

b) heat flux distribution.

Figure 4. The WRRM model testing in the UT-1M wind tunnel at α=50° , M=6 , Re≈9×10^6

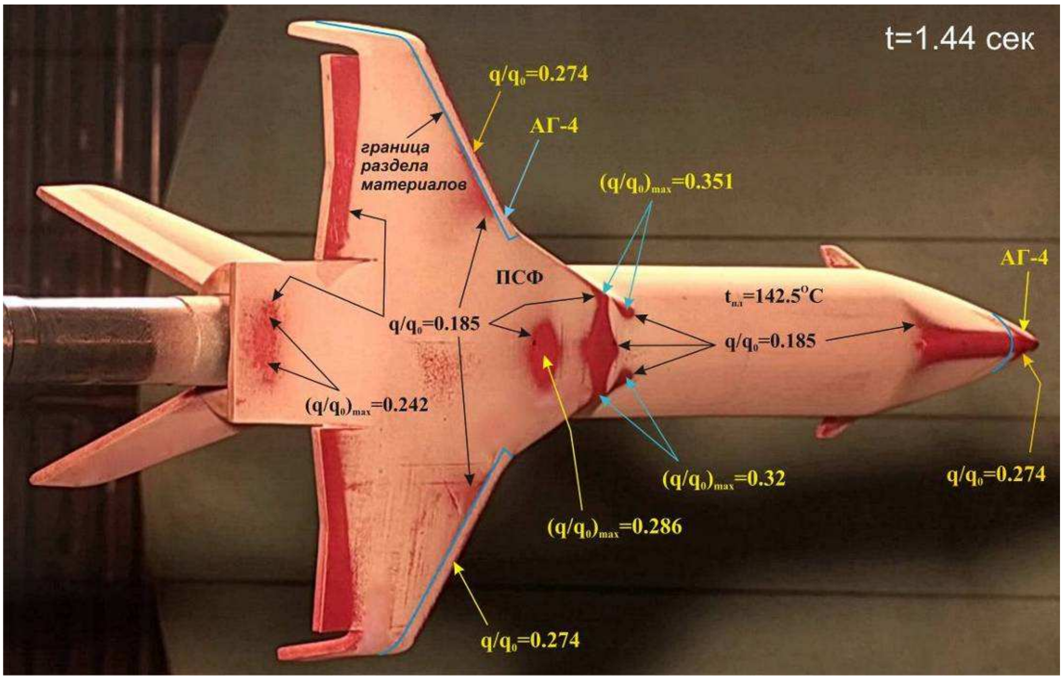

Figure 5. The WRRM model testing in the T-117 wind tunnel at α=50° , M=7.5 , Re≈2×10^6

Copyright Statement